Interpretation of the Cu K-edge EXAFS spectra of Cu_3N using ab initio molecular dynamics

Dmitry Bocharov[a,*], Andris Anspoks[a], Janis Timoshenko[b], Aleksandr Kalinko[c],
Matthias Krack[d], Alexei Kuzmin[a]

[a]*Institute of Solid State Physics, University of Latvia, Kengaraga street 8, LV-1063 Riga, Latvia*
[b]*Department of Materials Science and Chemical Engineering, Stony Brook University, Stony Brook, New York 11794, USA*
[c]*Department Chemie, Naturwissenschaftliche Fakultät, Universität Paderborn, Warburger Strasse 100, 33098 Paderborn, Germany*
[d]*Paul Scherrer Institut, Forschungsstrasse 111, 5232 Villigen PSI, Switzerland*

Abstract

Cubic copper nitride (Cu_3N) has anti-perovskite structure, and its properties are strongly affected by anisotropic thermal vibrations of copper atoms. *Ab initio* molecular dynamics (AIMD) simulations were performed in the temperature range from 300 K to 700 K in order to probe the details of Cu_3N lattice dynamics. The Cu K-edge extended X-ray absorption fine structure (EXAFS) spectrum of bulk Cu_3N was used to validate AIMD simulations at 300 K. The AIMD results suggest strong anharmonicity of the Cu–N and Cu–Cu bonds, the rigidity of NCu_6 octahedra and strong correlation in atomic motion within –N–Cu–N– atom chains as well as support anisotropy of copper thermal vibrations.

Keywords: Copper nitride, Cu_3N, Extended X-ray absorption fine structure (EXAFS), Ab initio molecular dynamics

*Corresponding author
  E-mail address:* bocharov@latnet.lv (Dmitry Bocharov).

D. Bocharov, A. Anspoks, J. Timoshenko, A. Kalinko, M. Krack, A. Kuzmin,

1. Introduction

Copper nitride (Cu_3N) has a cubic anti-ReO_3-type structure (Fig. 1) composed of the NCu_6 octahedra joined by corners (Zachwieja and Jacobs, 1990; Paniconi et al., 2007). Opposite to metallic ReO_3, pure Cu_3N is a narrow band gap (E_g=1.1–1.8 eV) semiconductor (Jiang et al., 2018). Cu_3N is potentially interesting candidate for many applications such as write-once read-many (WORM) optical storage devices (Asano et al., 1990; Maruyama and Morishita, 1996), non-volatile magnetic random access memories (Borsa et al., 2002) and optical lithography for a fabrication of microscopic metal links (Maya, 1993; Borsa and Boerma, 2004). Electro-catalytic properties of copper nitride in alkaline fuel cells were also reported (Wu and Chen, 2011). Cu_3N usage as an absorber for photovoltaic and photo-electrochemical solar cells was recently reported (Zakutayev et al., 2014; Caskey et al., 2014).

The dynamic properties of Cu_3N lattice are determined by anisotropic thermal vibrations of copper atoms, having larger amplitude orthogonal to linear –N–Cu–N– atomic chains (Zachwieja and Jacobs, 1990). X-ray absorption spectroscopy is ideally suited to probe in-situ local atomic structure and lattice dynamics of Cu_3N (Kuzmin et al., 2016b; Timoshenko et al., 2017). It was shown previously based on the results of reverse Monte Carlo calculations (Timoshenko et al., 2016, 2017) that the anisotropy of copper atom vibrations is enhanced upon increasing temperature and is accompanied by tilting motion of NCu_6 octahedra. Strong correlation in the motion of atoms was observed along –N–Cu–N– atomic chains but it reduced with an increase of interatomic distance. Finally, it was found that anticorrelated motion of nearest Cu atoms indicates on breathing-type motion of NCu_6 octahedra.

Another atomistic simulation approach to the interpretation of EXAFS utilizes molecular dynamics (MD) simulations (D'Angelo et al., 1994, 1996; Palmer et al., 1996). The MD-EXAFS method is especially useful for the analysis of EXAFS in crystalline materials where outer shell and multiple-scattering (MS) contributions are significant and overlap (Kuzmin and Evarestov, 2009; Kuzmin et al., 2016a; Bocharov et al., 2016). Besides, the method can be employed to validate the interatomic potential models used in the classical MD simulations (Kuzmin et al., 2016a; Bocharov et al.,

D. Bocharov, A. Anspoks, J. Timoshenko, A. Kalinko, M. Krack, A. Kuzmin,
Interpretation of the Cu K-edge EXAFS spectra of Cu3N using ab initio molecular dynamics,
Rad. Phys. Chem. 175 (2020) 108100.

2017).

In the MD-EXAFS method, the structural model of a material is constructed first, taking into account periodicity, chemical composition as well as the particle size and shape in the case of nanomaterials. One should also define the interaction potential model, which can be based on empirical force-field or calculated from first-principles. Next, the MD simulation is performed at the required temperature and pressure, providing a set of instantaneous atomic configurations ("snapshots"), which represent a time-dependent evolution of the material structure. The use of Newtonian dynamics restricts the application of MD at low temperatures, where the quantum zero-point motion of atoms becomes important. Nevertheless, MD method usually performs well at high temperatures and, thus, is suitable to model the anharmonic thermal motion of atoms. When the MD simulation is done, the accumulated coordinates of atoms can be used to evaluate different structural properties as, for example, the radial distribution functions, the mean interatomic distances and angles, the mean-square relative displacements, etc. Moreover, a set of EXAFS spectra can be calculated for each of the atomic configurations within ab initio MS formalism, and the configuration-averaged EXAFS spectrum can be readily compared with the experiment to validate the MD simulation.

The MD-EXAFS approach, based on classical MD simulations, has been successfully applied previously to a number of perovskite-type materials as $SrTiO_3$ (Kuzmin and Evarestov, 2009; Kuzmin et al., 2016a), ReO_3 (Kalinko et al., 2009), $LaCoO_3$ (Kuzmin et al., 2011) and ScF_3 (Bocharov et al., 2016). Some preliminary results have been also obtained for Cu_3N (Timoshenko et al., 2016).

In this study, we performed systematic *ab initio* molecular dynamics (AIMD) simulations of bulk Cu_3N in the temperature range from 300 K to 700 K in order to elucidate the details of lattice dynamics and anharmonicity of the Cu–N and Cu–Cu bonding.

2. Experimental

The room temperature Cu K-edge X-ray absorption spectrum (Fig. 2) of commercial polycrystalline Cu_3N powder (99.5%, Alfa Aesar) was acquired in transmission

3

mode at the bending magnet beamline C (Rickers et al., 2007) at HASYLAB/DESY synchrotron radiation facility. The details of the experiment and data treatment were published previously (Kuzmin et al., 2016b; Timoshenko et al., 2017).

3. Computational details

The AIMD simulations of bulk Cu_3N were performed based on Kohn-Sham density functional theory (DFT) within the isobaric-isothermal (NpT) ensemble. The QUICKSTEP module (VandeVondele et al., 2005) of the CP2K code (CP2K developers group, 2000–2018) was employed for all AIMD runs using the Cray XC50 system "Piz Daint" at the Swiss National Supercomputing Centre (CSCS). Goedecker-Teter-Hutter (GTH) pseudopotentials (semi-core GTH PP for Cu) (Krack, 2005) and contracted Gaussian basis sets of double-zeta quality specifically optimised for the use with the GTH pseudopotentials in the framework of CP2K for condensed phase systems (DZVP, MOLOPT-SR) (VandeVondele and Hutter, 2007) were employed in all runs.

NpT ensemble AIMD was conducted at four temperatures: 300, 450, 600, and 700 K. A thermalisation run of about 15 ps duration was performed at each temperature to equilibrate the supercell $5a_0 \times 5a_0 \times 5a_0$ (a_0=3.819 Å is the lattice parameter) Cu_3N model system with periodic boundary conditions at the actual target temperature. This supercell size is large enough to avoid artefacts in the EXAFS spectra during the MD-EXAFS analysis (Kuzmin and Evarestov, 2009) in the post-processing phase. Finally, the equilibrated systems were used in the production runs of about 30 ps duration at the each target temperature.

Sets of atomic coordinates obtained as a result of the AIMD simulations were used to calculate the radial distribution functions (RDFs) and the mean-square relative displacements (MSRD) (also known as Debye-Waller factors) for Cu–N and Cu–Cu atom pairs. The average bond angles and the bond angles between the average positions of Cu and N atoms were also evaluated.

Sets of atomic configurations obtained in the AIMD simulations were used to calculate the configuration-averaged Cu K-edge EXAFS $\chi(k)$ (k is the photoelectron wavenumber) within the multiple-scattering (MS) approach (Kuzmin and Evarestov,

2009; Kuzmin et al., 2016a) using *ab initio* self-consistent real-space MS FEFF8.50L code (Ankudinov et al., 1998; Rehr and Albers, 2000). The scattering potential and partial phase shifts were calculated only once for the cluster with the radius of 8 Å, centered at the absorbing Cu atom and constructed based on the crystallographic Cu_3N structure. The photoelectron inelastic losses were accounted using the complex exchange-correlation Hedin-Lundqvist potential (Hedin and Lundqvist, 1971).

4. Results

The experimental and calculated (using NpT ensemble AIMD) Cu K-edge EXAFS spectra of bulk Cu_3N at 300 K and their Fourier transforms (FTs) are compared in Fig. 2. The overall agreement between theory and experiment is quite good. The frequency of the EXAFS signals and the related positions of peaks in FTs are well reproduced by the simulations. However, the amplitudes of the FT peaks at 2.3 Å and 3.4 Å are larger in the simulated signal indicating that thermal disorder is underestimated in the second and third coordination shells.

Atomic configurations produced in the AIMD simulations of Cu_3N can be used to extract a number of structural parameters and their temperature dependencies.

In Fig. 3 the calculated radial distribution functions (RDFs) $G(R)$ around the absorbing atom Cu_0 are shown in the region of the nearest two shells, corresponding to Cu_0–N_1 and Cu_0–Cu_2 atom pairs. The asymmetric shape of the two peaks at ~1.9 Å and ~2.7 Å suggests a strong anharmonicity of the atomic vibrations in Cu_3N.

The temperature dependencies of the mean-square relative displacements (MSRD) for the first seven coordination shells of the absorbing Cu_0 atom are shown in Fig. 4 for Cu–N and Cu–Cu atom pairs. The results of reverse Monte Carlo (RMC) analysis of low-temperature (10-300 K) EXAFS data are also given for comparison (Timoshenko et al., 2017). The two sets of MSRD data match each other at 300 K. The temperature dependencies of the MSRD factors for Cu_0–N_1, Cu_0–N_4, Cu_0–Cu_2 and Cu_0–Cu_6 atom pairs agree well between low-temperature experimental and high-temperature calculated values. At the same time, the AIMD calculated MSRD factors for Cu_0–N_{7b}, Cu_0–Cu_{3b} and Cu_0–Cu_5 atom pairs are overestimated, but for Cu_0–N_{7a} and Cu_0–Cu_{3b}

atom pairs are slightly underestimated. Thus, overall, the AIMD calculations are able to describe the structure and dynamics of bulk Cu_3N.

It is important that analysis of atomic coordinates allows us to separate atom pairs having similar interatomic distances as Cu_0–N_{7a} and Cu_0–N_{7b} or Cu_0–Cu_{3a} and Cu_0–Cu_{3b} (Fig. 1). Small values of MSRDs for Cu–N_1, Cu–Cu_{3a} and Cu–N_{7a} atom pairs relative to others suggest strong correlation in atomic motion along crystallographic axes within –Cu–N–Cu–N– atomic chains. Moreover, the MSRD factors for Cu_0–Cu_{3b} are much larger than those for Cu_0–Cu_{3a} indicating anisotropic thermal vibration of Cu atoms, with the amplitude being larger in the direction orthogonal to –N–Cu–N– chains.

Temperature dependencies of several bond angles are shown in Figs. 5, 6 and 7. Here we distinguish between the average values of bond angles ($\langle\rangle$), seen by EXAFS, and the angle values between the average positions of atoms ($\langle\rangle$-$\langle\rangle$-$\langle\rangle$), seen by diffraction. A strong difference between these two cases was observed for N_1–Cu_{3a}–N_{7a}, Cu_0–N_1–Cu_{3a} and Cu_0–Cu_2–Cu_6 angles, whereas no or very small difference was detected for Cu_0–N_1–Cu_2 and Cu_0–Cu_2–Cu_{3a} angles.

The anisotropic vibrational amplitude of Cu atoms is responsible for a decrease of the average values of N_1–Cu_{3a}–N_{7a} and Cu_0–N_1–Cu_{3a} angles by about 5–15°. At the same time, the rigidity of NCu_6 octahedra is supported by a stability of Cu_0–N_1–Cu_2 and Cu_0–Cu_2–Cu_{3a} angles being close to 90°. Finally, a dynamical tilting of NCu_6 octahedra can be deduced from a behaviour of Cu_0–Cu_2–Cu_6 angle together with the large MSRD for Cu_0–Cu_{3b}.

5. Conclusion

Ab initio molecular dynamics simulations of cubic anti-perovskite copper nitride were performed within the NpT ensemble in the temperature range between 300 and 700 K. The AIMD results were validated using the MD-EXAFS approach by direct comparison with the Cu K-edge EXAFS of polycrystalline Cu_3N at 300 K. The simulations predict strong anharmonicity of Cu–N and Cu–Cu bonds, anisotropy of Cu atoms vibrations, the rigidity of NCu_6 octahedra and strong correlation in atomic mo-

tion within –N–Cu–N– atom chains. These findings are in agreement with the reverse Monte Carlo analysis of low-temperature (10–300 K) EXAFS data (Timoshenko et al., 2017).

6. Acknowledgements

References

Ankudinov, A.L., Ravel, B., Rehr, J.J., Conradson, S.D., 1998. Real-space multiple-scattering calculation and interpretation of X-ray-absorption near-edge structure. Phys. Rev. B 58, 7565–7576. doi:10.1103/PhysRevB.58.7565.

Asano, M., Umeda, K., Tasaki, A., 1990. Cu_3N thin film for a new light recording media. Jap. J. Appl. Phys. 29, 1985. doi:1347-4065/29/i=10R/a=1985.

Bocharov, D., Chollet, M., Krack, M., Bertsch, J., Grolimund, D., Martin, M., Kuzmin, A., Purans, J., Kotomin, E., 2017. Analysis of the U L_3-edge X-ray absorption spectra in UO_2 using molecular dynamics simulations. Prog. Nucl. Energy 94, 187–193. doi:10.1016/j.pnucene.2016.07.017.

Bocharov, D., Krack, M., Kalinko, A., Purans, J., Rocca, F., Ali, S.E., Kuzmin, A., 2016. Ab initio molecular dynamics simulations of the Sc K-edge EXAFS of scandium trifluoride. J. Phys.: Conf. Ser. 712, 012009. doi:10.1088/1742-6596/712/1/012009.

Borsa, D., Boerma, D., 2004. Growth, structural and optical properties of Cu_3N films. Surf. Sci. 548, 95–105. doi:10.1016/j.susc.2003.10.053.

Borsa, D.M., Grachev, S., Presura, C., Boerma, D.O., 2002. Growth and properties of Cu$_3$N films and Cu$_3$N/$\gamma\prime$-Fe$_4$N bilayers. Appl. Phys. Lett. 80, 1823–1825. doi:10.1063/1.1459116.

Caskey, C.M., Richards, R.M., Ginley, D.S., Zakutayev, A., 2014. Thin film synthesis and properties of copper nitride, a metastable semiconductor. Mater. Horiz. 1, 424–430. doi:10.1039/C4MH00049H.

CP2K developers group, 2000–2018. (http://www.cp2k.org).

D'Angelo, P., Di Nola, A., Filipponi, A., Pavel, N.V., Roccatano, D., 1994. An extended x-ray absorption fine structure study of aqueous solutions by employing molecular dynamics simulations. J. Chem. Phys. 100, 985–994. doi:10.1063/1.466581.

D'Angelo, P., Di Nola, A., Mangoni, M., Pavel, N.V., 1996. An extended x-ray absorption fine structure study by employing molecular dynamics simulations: Bromide ion in methanolic solution. J. Chem. Phys. 104, 1779–1790. doi:10.1063/1.471711.

Hedin, L., Lundqvist, S., 1971. Explicit local exchange-correlation potentials. J. Phys. C: Solid State Phys. 4, 2064. doi:10.1088/0022-3719/4/14/022.

Jiang, A., Qi, M., Xiao, J., 2018. Preparation, structure, properties, and application of copper nitride (Cu$_3$N) thin films: A review. J. Mater. Sci. Technol. 34, 1467–1473. doi:10.1016/j.jmst.2018.02.025.

Kalinko, A., Evarestov, R.A., Kuzmin, A., Purans, J., 2009. Interpretation of EXAFS in ReO$_3$ using molecular dynamics simulations. J. Phys.: Conf. Ser. 190, 012080. doi:10.1088/1742-6596/190/1/012080.

Krack, M., 2005. Pseudopotentials for H to Kr optimized for gradient-corrected exchange-correlation functionals. Theor. Chem. Acc. 114, 145–152. doi:10.1007/s00214-005-0655-y.

Kuzmin, A., Anspoks, A., Kalinko, A., Timoshenko, J., 2016a. The use of X-ray absorption spectra for validation of classical force-field models. Z. Phys. Chem. 230, 537–549. doi:10.1515/zpch-2015-0664.

Kuzmin, A., Efimov, V., Efimova, E., Sikolenko, V., Pascarelli, S., Troyanchuk, I., 2011. Interpretation of the Co K-edge EXAFS in LaCoO$_3$ using molecular dynamics simulations. Solid State Ionics 188, 21–24. doi:10.1016/j.ssi.2010.09.036.

Kuzmin, A., Evarestov, R.A., 2009. Quantum mechanics–molecular dynamics approach to the interpretation of x-ray absorption spectra. Journal of Physics: Condensed Matter 21, 055401. doi:10.1088/0953-8984/21/5/055401.

Kuzmin, A., Kalinko, A., Anspoks, A., Timoshenko, J., Kalendarev, R., 2016b. Study of copper nitride thin film structure. Latvian J. Phys. Tech. Sci. 53, 31–37. doi:10.1515/lpts-2016-0011.

Maruyama, T., Morishita, T., 1996. Copper nitride and tin nitride thin films for write-once optical recording media. Appl. Phys. Lett. 69, 890–891. doi:10.1063/1.117978.

Maya, L., 1993. Deposition of crystalline binary nitride films of tin, copper, and nickel by reactive sputtering. J. Vacuum Sci. Technol. A 11, 604–608. doi:10.1116/1.578778.

Palmer, B.J., Pfund, D.M., Fulton, J.L., 1996. Direct modeling of exafs spectra from molecular dynamics simulations. J. Chem. Phys. 100, 13393–13398. doi:10.1021/jp960160q.

Paniconi, G., Stoeva, Z., Doberstein, H., Smith, R.I., Gallagher, B.L., Gregory, D.H., 2007. Structural chemistry of Cu$_3$N powders obtained by ammonolysis reactions. Solid State Sci. 9, 907–913. doi:10.1016/j.solidstatesciences.2007.03.017.

Rehr, J.J., Albers, R.C., 2000. Theoretical approaches to X-ray absorption fine structure. Rev. Mod. Phys. 72, 621–654. doi:10.1103/RevModPhys.72.621.

Rickers, K., Drube, W., Schulte-Schrepping, H., Welter, E., Brüggmann, U., Herrmann, M., Heuer, J., Schulz-Ritter, H., 2007. New XAFS facility for in-situ measurements at beamline C at HASYLAB. AIP Conf. Proc. 882, 905–907. doi:10.1063/1.2644700.

Timoshenko, J., Anspoks, A., Kalinko, A., Kuzmin, A., 2016. Local structure of copper nitride revealed by EXAFS spectroscopy and a reverse Monte Carlo/evolutionary algorithm approach. Phys. Scr. 91, 054003. doi:10.1088/0031-8949/91/5/054003.

Timoshenko, J., Anspoks, A., Kalinko, A., Kuzmin, A., 2017. Thermal disorder and correlation effects in anti-perovskite-type copper nitride. Acta Mater. 129, 61–71. doi:10.1016/j.actamat.2017.02.074.

VandeVondele, J., Hutter, J., 2007. Gaussian basis sets for accurate calculations on molecular systems in gas and condensed phases. J. Chem. Phys. 127, 114105. doi:10.1063/1.2770708.

VandeVondele, J., Krack, M., Mohamed, F., Parrinello, M., Chassaing, T., Hutter, J., 2005. QUICKSTEP: Fast and accurate density functional calculations using a mixed Gaussian and plane waves approach. Comput. Phys. Commun. 167, 103–128. doi:10.1016/j.cpc.2004.12.014.

Wu, H., Chen, W., 2011. Copper nitride nanocubes: Size-controlled synthesis and application as cathode catalyst in alkaline fuel cells. J. Am. Chem. Soc. 133, 15236–15239. doi:10.1021/ja204748u.

Zachwieja, U., Jacobs, H., 1990. Ammonothermalsynthese von kupfernitrid, Cu_3N. J. Less Common Metals 161, 175–184. doi:10.1016/0022-5088(90)90327-G.

Zakutayev, A., Caskey, C.M., Fioretti, A.N., Ginley, D.S., Vidal, J., Stevanovic, V., Tea, E., Lany, S., 2014. Defect Tolerant Semiconductors for Solar Energy Conversion. J. Phys. Chem. Lett. 5, 1117–1125. doi:10.1021/jz5001787.
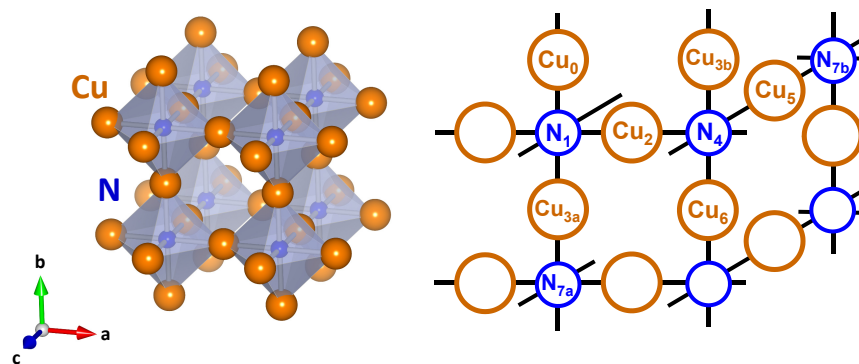
Figure 1: Crystal structure of cubic Cu_3N composed of regular NCu_6 octahedra (left panel). Fragment of Cu_3N structure with the labelled atoms of the first seven coordination shells around the absorbing copper atom Cu_0 (right panel). Non-equivalent atoms located at the same distance from the absorbing one are denoted by (a) and (b).
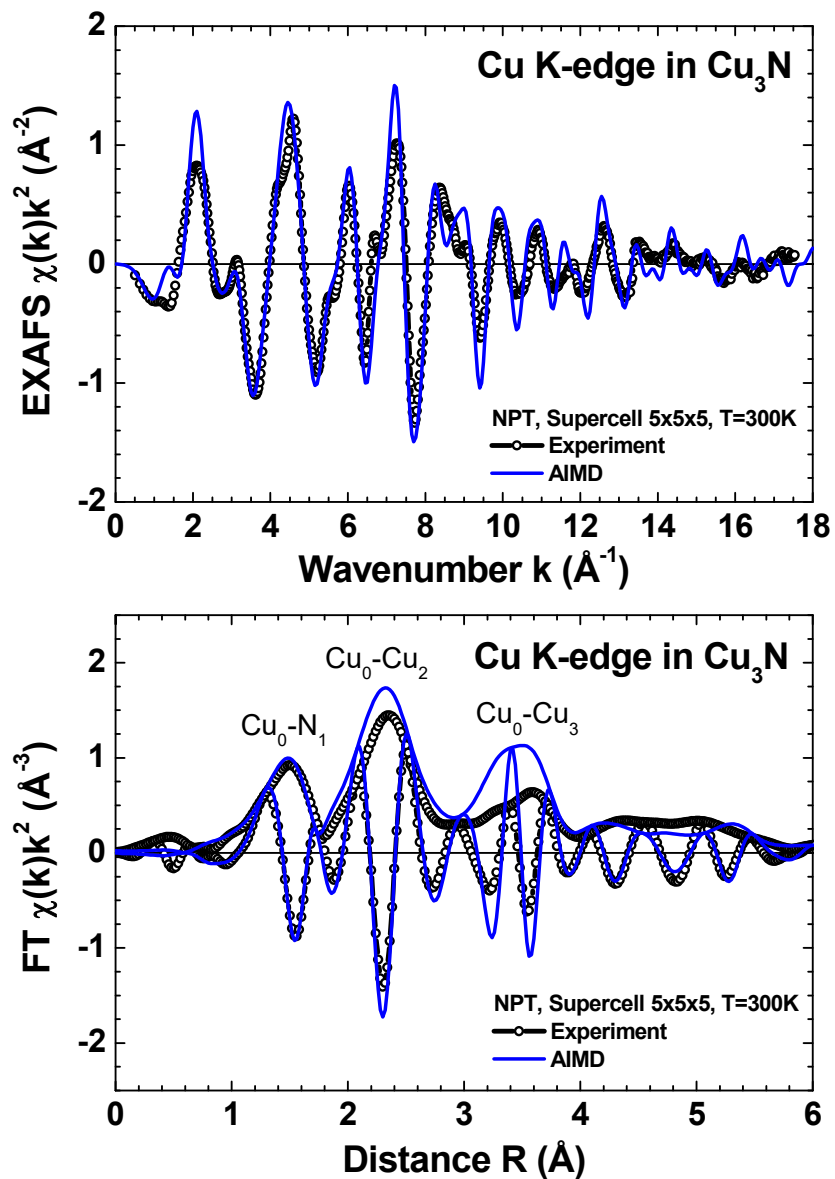
Figure 2: The experimental and AIMD calculated Cu K-edge EXAFS spectra (top panel) and their Fourier transforms (FTs) (bottom panel) at 300 K. The three peaks in FTs corresponding to the three nearest coordination shells, composed of nitrogen and copper atoms are indicated.
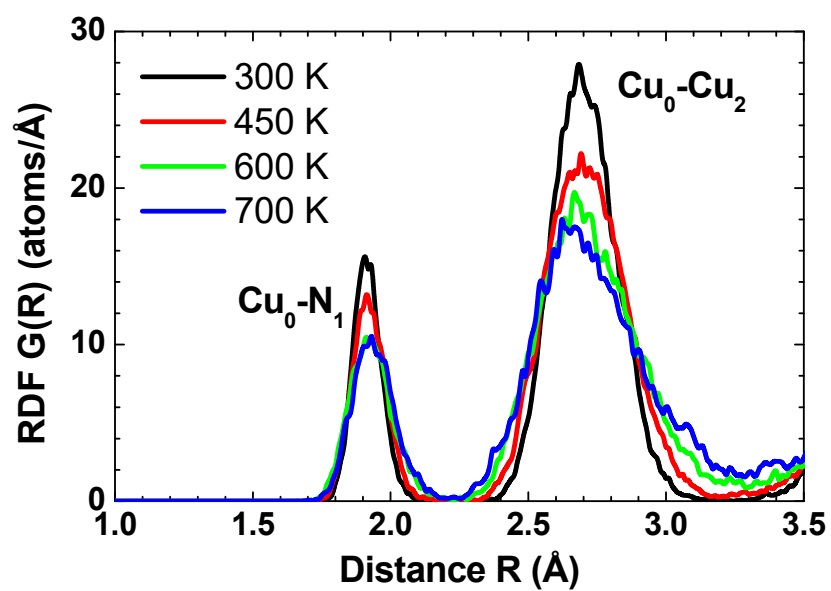
Figure 3: Temperature dependence of the radial distribution functions for Cu_0–N_1 and Cu_0–Cu_2 atom pairs obtained from AIMD simulations. Note pronounced asymmetry of both RDFs due to anharmonic lattice dynamics in Cu_3N.
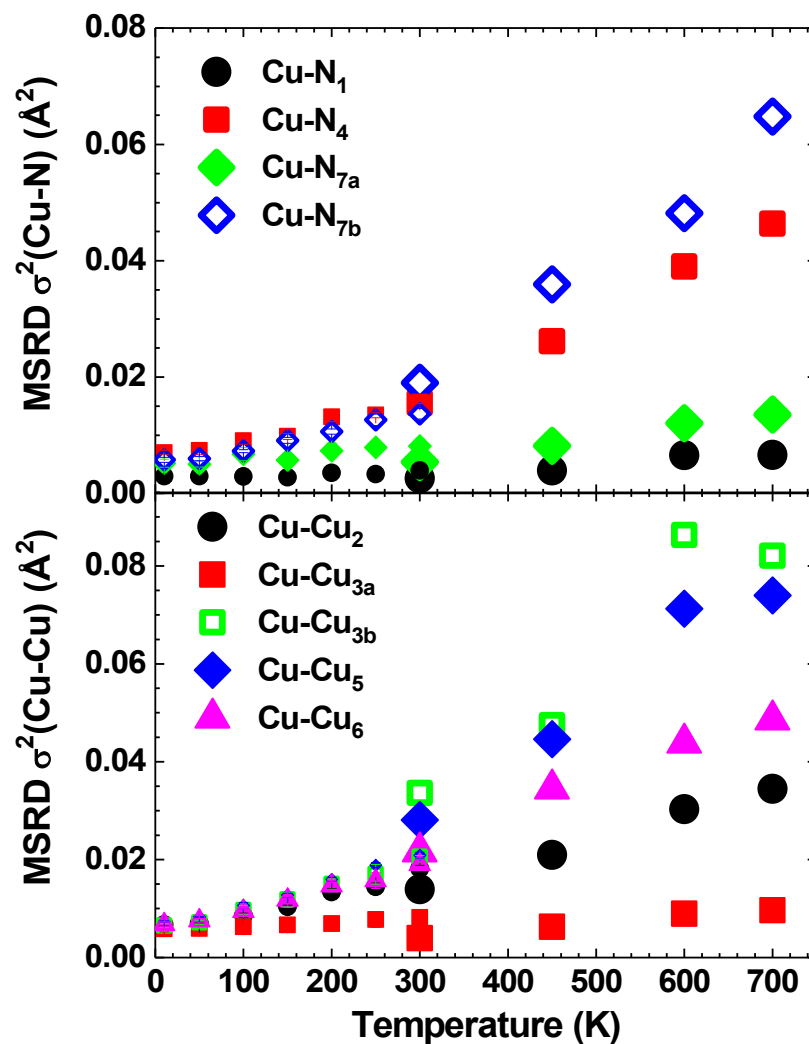
Figure 4: Temperature dependencies of the MSRD factors calculated from the results of AIMD simulations for Cu–N (top panel) and Cu–Cu (bottom panel) atom pairs in the first seven coordination shells around the absorbing (Cu$_0$) atoms at four different temperatures (300, 450, 600 and 700 K). The MSRD values shown by small symbols are taken from reverse Monte Carlo analysis of low-temperature (10-300 K) EXAFS data (Timoshenko et al., 2017).
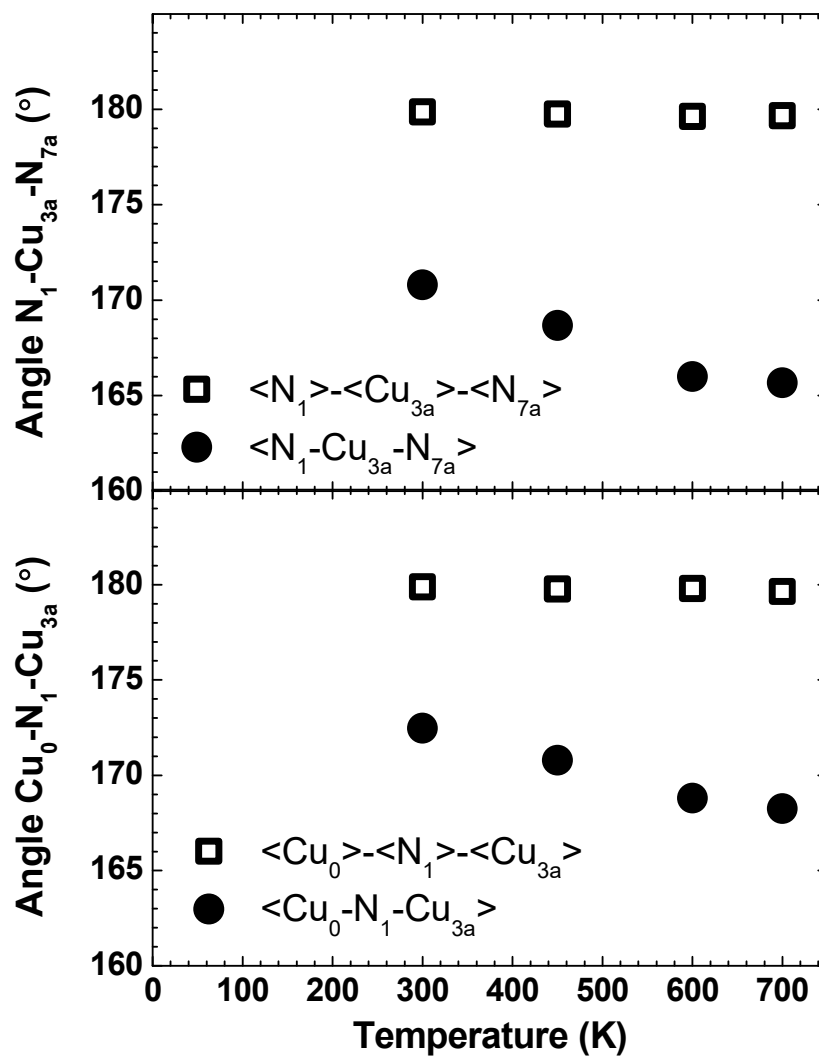
Figure 5: Temperature dependencies of the N_1–Cu_{3a}–N_{7a} and Cu_0–N_1–Cu_{3a} bond angle values in Cu_3N system. Open squares are angles between the average positions of atoms, whereas solid circles correspond to the average angles.
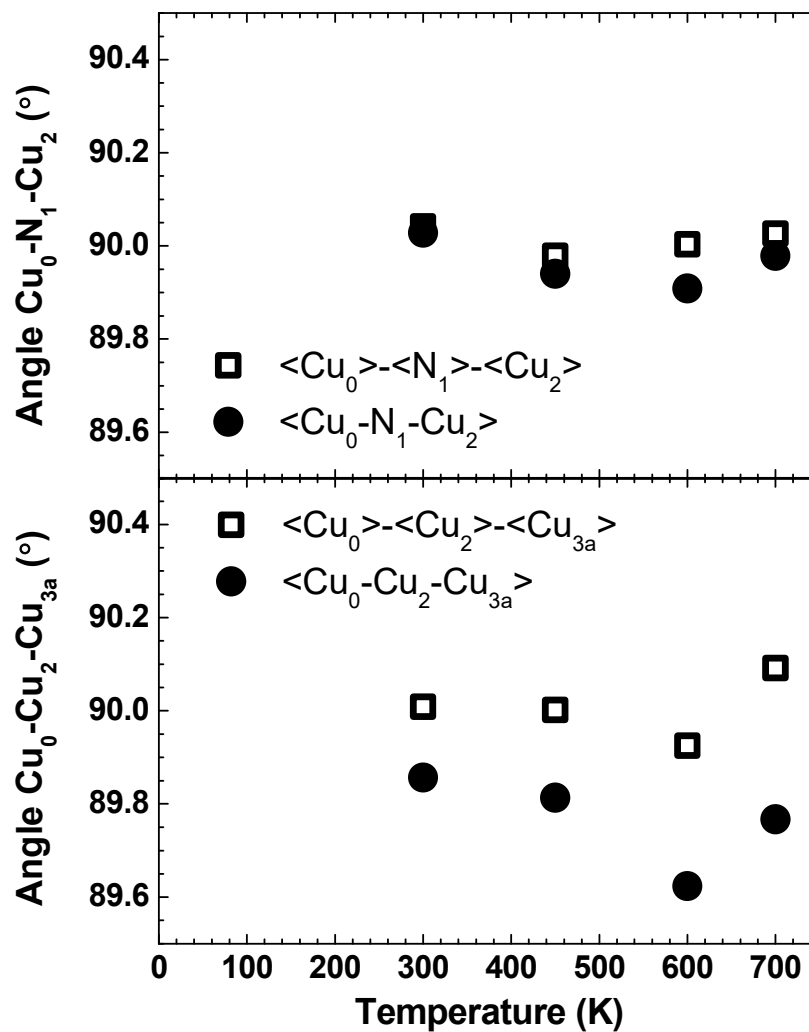
Figure 6: Temperature dependencies of the Cu_0–N_1–Cu_2 and Cu_0–Cu_2–Cu_{3a} bond angle values in Cu_3N system. Open squares are angles between the average positions of atoms, whereas solid circles correspond to the average angles.
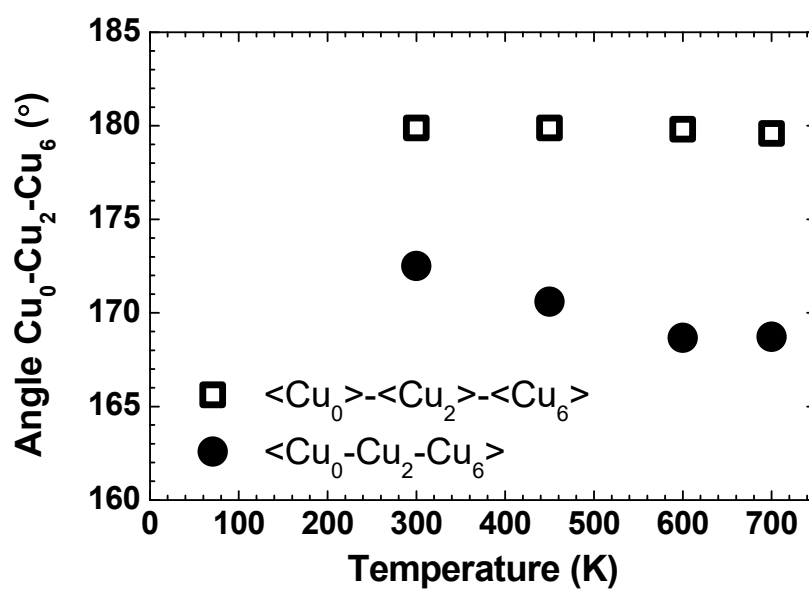
D. Bocharov, A. Anspoks, J. Timoshenko, A. Kalinko, M. Krack, A. Kuzmin,
Interpretation of the Cu K-edge EXAFS spectra of Cu3N using ab initio molecular dynamics,
Rad. Phys. Chem. 175 (2020) 108100.

Figure 7: Temperature dependencies of the Cu_0–Cu_2–Cu_6 bond angle values in for atoms in in Cu_3N system.
Open squares are angles between the average positions of atoms, whereas solid circles correspond to the
average angles.